Biomaterials Science

PAPER

View Article Online
View Journal | View Issue

Cite this: *Biomater. Sci.*, 2018, **6**, 388

The uptake, retention and clearance of drug-loaded dendrimer nanoparticles in astrocytes – electrophysiological quantification†

Helena H. Chowdhury, ‡[a,b] Susana R. Cerqueira,‡[c,d,e] Nuno Sousa,[d,e] Joaquim M. Oliveira,[c,e] Rui L. Reis[c,e] and Robert Zorec*[a,b]

Nanoparticle-based drug delivery systems may impose risks to patients due to potential toxicity associated with a lack of clearance from cells or prolonged carrier-cell retention. This work evaluates vesicular cell uptake, retention and the possible transfer of endocytosed methylprednisolone-loaded carboxymethylchitosan/poly(amidoamine) dendrimer nanoparticles (NPs) into secretory vesicles of rat cultured astrocytes. The cells were incubated with NPs and unitary vesicle fusions/fissions with the plasma membrane were monitored employing high-resolution membrane capacitance measurements. In the NP-treated cells the frequency of unitary exocytotic events was significantly increased. The presence of NPs also induces an increase in the size of exocytotic vesicles interacting with the plasma membrane, which exhibit transient fusion with prolonged fusion pore dwell-time. Live-cell confocal imaging revealed that once NPs internalize into endocytotic compartments they remain in the cell for 7 days, although a significant proportion of these merge with secretory vesicles destined for exocytosis. Co-localization studies show the route of clearance of NPs from cells *via* the exocytotic pathway. These findings bring new insight into the understanding of the intracellular trafficking and biological interactions of drug-loaded dendrimer NPs targeting astrocytes.

Received 29th September 2017,
Accepted 22nd December 2017

DOI: 10.1039/c7bm00886d

rsc.li/biomaterials-science

1. Introduction

Nanoparticle (NP) systems are emerging as new delivery carriers for pharmacological substances in biomedical applications.[1] NP-based systems are being engineered to deliver low-molecular-weight molecules efficiently to target tissues and/or subcellular compartments.[2] Various nanostructures have been tested as carriers in drug delivery systems, including liposomes, polymers, magnetic nanoparticles, silicon or carbon materials, and dendrimers.[3,4] Dendrimers are a class of polymeric NPs with unique architectures, exhibiting highly branched spherical structures,[5,6] and are useful because of their adjustable chemistry, allowing fine-tuning of their properties including a variety of functionalization and surface engineering possibilities.[7] Although it has recently become evident that the physical and chemical properties of dendrimers have a considerable effect on the interaction with cells, particularly cell internalization and trafficking mechanisms,[8–10] there are still only a few reports addressing the interplay between dendrimers and cell membranes and intracellular trafficking.[11] Experiments on poly(amidoamine) (PAMAM) dendrimers with carboxymethylchitosan (*CM*Cht), incorporating the therapeutic lipophilic drug, methylprednisolone (MP),[12–14] revealed their potential for use as nanocarriers in the central nervous system (CNS) for conditions targeting injured neural tissue.[15,16] However, how these NPs interact with neuroglia, homeostatically supporting neuronal networks and contributing to the maintenance of the blood–brain barrier, has not yet been addressed.

In the present study, we investigated the properties of *CM*Cht/PAMAM dendrimer NP interactions with the astrocyte plasma membrane using high-resolution real-time patch-clamp electrophysiology capacitance measurements and combined this technique with live-cell confocal imaging.

[a]*Laboratory of Neuroendocrinology – Molecular Cell Physiology, Institute of Pathophysiology, Faculty of Medicine, Zaloška 4, 1000 Ljubljana, Slovenia. E-mail: robert.zorec@mf.uni-lj.si; Tel: +386 1 543 7080*
[b]*Celica Biomedical, Tehnološki Park 24, Ljubljana, Slovenia*
[c]*3B's Research Group – Biomaterials, Biodegradables and Biomimetics, University of Minho, Headquarters of the European Institute of Excellence on Tissue Engineering and Regenerative Medicine, AvePark, Zona Industrial da Gandra, 4805-017 Barco GMR, Portugal*
[d]*Life and Health Sciences Research Institute (ICVS), School of Health Sciences, University of Minho, 4710-057 Braga, Portugal*
[e]*ICVSICVS/3B's – PT Government Associate Laboratory, Braga/Guimarães, Portugal*
†Electronic supplementary information (ESI) available. See DOI: 10.1039/c7bm00886d
‡These authors contributed equally to this work.

Membrane capacitance (C_m) is a parameter linearly related to the membrane area, the fluctuations of which mirror the interaction of single vesicles with the plasma membrane as discrete step increases and decreases in C_m, reflecting endocytotic and exocytotic events, respectively.[17,18] This approach allows the quantification of the vesicle diameter of single endocytotic and exocytotic events and the mode of interaction of the vesicle with the plasma membrane. It also allows the occurrence of vesicle fission/fusion with the plasma membrane to be quantified. Thus, measurements of C_m represent an ideal approach to study how NPs affect this process directly at the single-vesicle level in a living cell. In contrast, vesicle trafficking studies using confocal microscopy imaging enables single vesicles labelled by fluorescent probes to be visualized and the co-localization coefficients of NPs with membrane structures were assessed. By studying the co-localization of distinct fluorescent markers within vesicles, the merger between intercellular vesicular compartments in a living cell can be studied.[19]

2. Experimental

2.1. *CM*Cht/PAMAM dendrimer nanoparticle synthesis and functionalization

*CM*Cht/PAMAM dendrimer NPs were produced as previously reported.[13] For a brief description see the ESI.†

2.2. Primary astrocyte cultures

Primary cultures of cortical astrocytes were prepared from newborn P3 Wistar rats.[20] The experiments on isolated cells were approved by the Veterinary Administration of the Republic of Slovenia (Permit no. U34401-48/2014/7) and the care of the experimental animals was in accordance with International Guiding Principles for Biomedical Research Involving Animals, which was developed by the Council for International Organizations of Medical Sciences and Directive on Conditions for issue of License for Animal Experiments for Scientific Research Purposes (Official Gazette of the Republic of Slovenia, no. 38/13). After tissue dissection, the isolated cells were plated out and grown in high glucose Dulbecco's modified Eagle's medium (DMEM), supplemented with fetal bovine serum (FBS, 10%), L-glutamine (2 mM), sodium pyruvate (1 mM) and penicillin/streptomycin. The cultures were maintained at 37 °C in 95% air/5% CO_2. The astrocytes were then sub-cultured onto 22 mm diameter poly-L-lysine-coated glass coverslips at low densities. Control cultures were grown in normal astrocyte culture medium and stimulated cells were incubated with astrocyte media supplemented with 200 μg mL^{-1} *CM*Cht/PAMAM dendrimer NPs for 6, 12 or 24 h before analysis. All reagents were purchased from Sigma-Aldrich, Germany.

2.3. Electrophysiological experiments

Cell-attached high-resolution membrane capacitance measurements were performed to record the real and imaginary parts of the admittance of the equivalent electrical circuit.[17] The imaginary part of admittance is proportional to the membrane C_m, a parameter linearly related to the membrane area. In the compensated mode of recording, one of the two outputs of the dual-phase lock-in amplifier signal is directly proportional to the changes in C_m.[21] Positive steps in C_m were interpreted as single exocytotic events and negative steps as single endocytotic events.[17] The amplitude and frequency of the steps in C_m were measured. Single astrocytes, revealing a typical star-like morphology, were chosen for the patch-clamp analysis. Recordings were made considering three different conditions: (1) control astrocytes grown in regular medium and recorded in ECS; (2) astrocytes cultured in regular medium and recorded with the membrane exposed to a pipette filled with a solution of *CM*Cht/PAMAM dendrimer NPs, designated as acute NP exposure; and (3) astrocytes incubated with the *CM*Cht/PAMAM dendrimer NPs for 24 hours; the cells were washed with ECS and membrane capacitance measurements were performed when the astrocytes were in ECS and the pipette solution contained ECS only. Off-line data analyses were performed using MATLAB software (MathWorks Inc.). For more details see the ESI.†

2.4. Vesicle labeling and live confocal imaging of astrocytes

Co-localization studies on live astrocytes were performed in order to identify whether both the endocytotic and exocytotic vesicles were affected by exposure to NPs. We also tested whether the NPs entered the endocytotic vesicles, as well as the exocytotic membrane compartment. Low-density astrocyte cultures pre-incubated with fluorescently labeled NPs for different periods of time were incubated with Alexa Fluor 546 dextran (Molecular Probes, USA) for 1.5 h and washed thoroughly using ECS before observation. In parallel experiments, to observe exocytotic vesicles, sub-confluent astrocyte cultures were transfected with the plasmid DNA encoding NPY tagged with NPY-mCherry. The cells were concomitantly incubated with fluorescently labeled NPs for different periods of time. Live confocal microscopy images were acquired with an inverted microscope (Zeiss LSM META 510, Germany). For more details see the ESI.†

2.5. Data analysis

Electrophysiological analysis was performed using CellAnn software for MATLAB (MathWorks, USA). Individual steps, both positive and negative, in the imaginary part of the admittance signal (with no projections in the direct current trace) were registered and counted as endocytotic, transient or full-fusion exocytotic events for the frequency determination. Vesicle diameters were calculated from measurements of the amplitude of discrete C_m events, assuming a spherical geometry of the vesicle and using a specific membrane capacitance of 8 fF μm^{-2}. Similarly, the vesicle pore opening time (dwell time or plateau phase) was also obtained from C_m recordings as the time of a reversible event at half maximal amplitude. The values are presented as means ± SEM unless stated otherwise. One-way analysis of variance and Student's t test were used as appropriate to assess statistical significance. Relative

co-localization of FITC-labelled NPs with Alexa Fluor 546 dextran and with NPY-mCherry, respectively, was quantified using ColocAna software (Celica, Slovenia). The co-localization was calculated as a percentage of co-localized pixels *versus* all above threshold pixels of the fluorescent NPs. The threshold intensity for the co-localized pixel count was 20% of the maximal fluorescence.

3. Results

To test whether the exposure of astrocytes to NPs alters the frequency of unitary fusion/fission events, we monitored changes in membrane capacitance (C_m) in NP-stimulated cells, either immediately after stimulation (acute condition) or after a 24 h incubation period. During the acute NP application (placing NPs into the patch-pipette solution), we considered the instant exposure of the astrocyte membrane to NPs during the recording; the prolonged stimulation condition consisted of pre-exposure to NPs for 24 h and then recording C_m in the absence of NPs. In both cases, 200 μg mL^{-1} NPs were used because there was no cytotoxicity recorded at this concentration.[22] A total of 20 astrocyte membrane patches were recorded for about 7 min on average. Three types of discrete events in C_m were observed: (1) single irreversible downward steps, indicating the occurrence of an endocytotic event; (2) transient (reversible) exocytotic events, consisting of a discrete increase followed by a decrease in C_m of similar amplitude within 3 s, illustrating transient vesicle fusion pore opening; and (3) discrete irreversible upward steps, representing full-fusion exocytotic events, as observed previously (Fig. 1A).[17,18,23,24]

3.1. Exposure of astrocytes to NPs increases the rate of endocytosis

Our data revealed that acute NP exposure of the astrocyte membrane *via* the patch-pipette solution tends to increase the frequency of endocytotic vesicle formation in the astrocyte membrane from 0.015 ± 0.003 events per s (n = 10, Fig. 1Bi) in controls to 0.031 ± 0.008 events per s (n = 7) under acute conditions or after 24-hour exposure (0.026 ± 0.003 events per s; n = 3). Although not strongly statistically significant (P = 0.103, ANOVA), a visible increase in the rate of endosome formation occurs after the exposure of astrocytes to NPs. In contrast to previous studies where the internalization of the *CM*Cht/PAMAM dendrimer NPs was detected only after 12 h of incubation, reaching the maximum intracellular load 24 h after exposure,[13] this study revealed changes in vesicle trafficking immediately upon exposure of astrocytes to NPs. These results suggest that the presence of NPs *per se* may stimulate endocytosis.

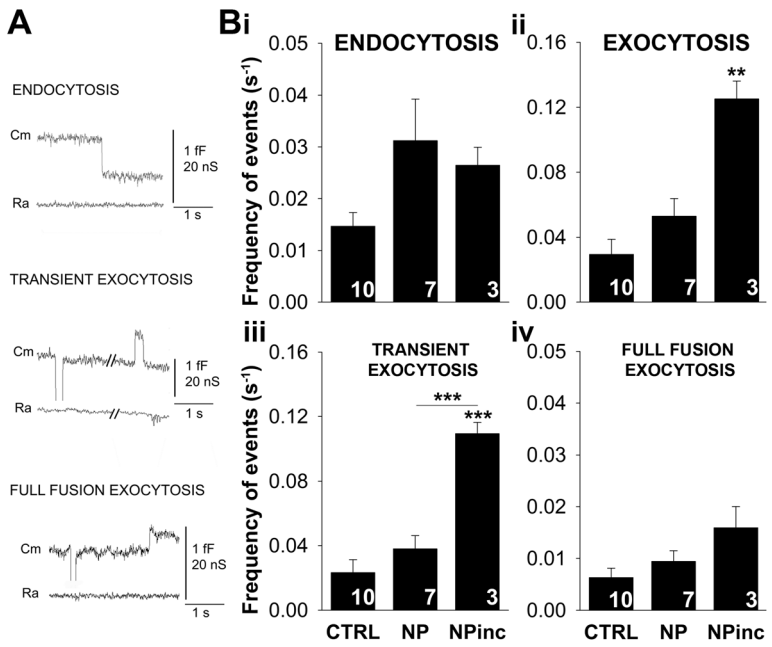

Fig. 1 Frequency of endocytotic and exocytotic events. (A) Representative recordings of an irreversible downward step in the imaginary admittance trace (C_m, proportional to the patch membrane area) (top panel, representing a unitary endocytotic event); a transient upward step (middle panel, transient exocytosis); and an irreversible upward step (bottom panel, full-fusion exocytotic event) recorded in the cell-attached mode of recording. Real parts of admittance trace (R_a). (B) Average frequency of endocytotic (Bi) and exocytotic (Bii) events in single astrocytes cultured in regular media (CTRL), exposed to NPs in the patch-pipette solution during the recording (NP) and after 24 h of incubation with NPs, washed and recorded in ECS (NPinc). Exocytotic events are further analysed, discriminating between transient (Biii) and full-fusion (Bvi) events. Values are presented as means ± SEM; the numbers in the columns represent the number of cells analysed. The significant differences compared with the respective control or between experimental groups are denoted as $^{**}P < 0.01$ and $^{***}P < 0.001$.

3.2. The rate of exocytosis increases following 24 hour incubation of astrocytes with NPs

We monitored the frequency of vesicle fusion by monitoring discrete upward steps in C_m. The results show that NP-incubated astrocytes exhibited a significantly higher rate of exocytotic events (0.125 ± 0.011 events per s; P = 0.009, ANOVA) than control cells (0.029 ± 0.009 events per s; Fig. 1Bii), whereas acute NP exposure only slightly increased the frequency of exocytosis compared with control cells (0.053 ± 0.011 events per s; P = 0.088, t test). These alterations indicate that NPs augment the transport of exocytotic vesicles and may also facilitate the clearance of NPs from cells, if NPs are present in secretory vesicles.

To further dissect exocytotic mechanisms in astrocytes after interaction with NPs, making a distinction between full-fusion and transient exocytotic events, we analysed the incidence of exocytosis before and after the addition of NPs to the astrocytes. Our findings revealed a strong prevalence of transient exocytosis for all the conditions tested (>70%, Table 1, ESI†). Although not statistically significant, the addition of NPs to the astrocytes increased the proportion of transient exocytotic fusion even more. As expected, astrocytes incubated with NPs exhibited a similar significantly higher rate of transient exocytotic events (0.109 ± 0.012 events per s) compared with control cells (0.023 ± 0.008 events per s; P < 0.001, ANOVA; Fig. 1Biii) and even compared with cells with acute NP exposure (0.038 ± 0.008 events per s; P < 0.001, ANOVA). In the full-fusion type of exocytotic events (Fig. 1Biv), the results show similar trends; the frequency of exocytosis increases after 24 h of incubation with NPs (P = 0.067).

In general, the results revealed changes in the frequency of endocytosis and exocytosis after NP stimulation and, as suggested in the literature, they seem to be occurring simultaneously and in a dynamic fashion as a consequence of interaction between the NPs and the plasma membrane.[25]

3.3. The presence of NPs increases vesicle size and fusion pore dwell time

Essentially, exposure of cells to NPs seems to have no effect on the size of endocytotic vesicles interacting with the plasma membrane; the mean vesicle size was almost the same in all three experimental conditions (138 ± 6 nm in controls; 138 ± 12 nm in NPs and 138 ± 5 nm in incubation with NPs; Fig. 2A). Although these results are consistent with the endocytotic pathway transporting the 109 nm diameter NPs to the astrocyte cytosol,[14,26] it seems that NPs do not *per se* activate a different type of endocytosis from that present in the controls. However, if we further analyse the results of endocytotic vesicle diameter and closely observe the frequency distribution of vesicle diameter histograms (Fig. 3, left panels), there is an evident shift

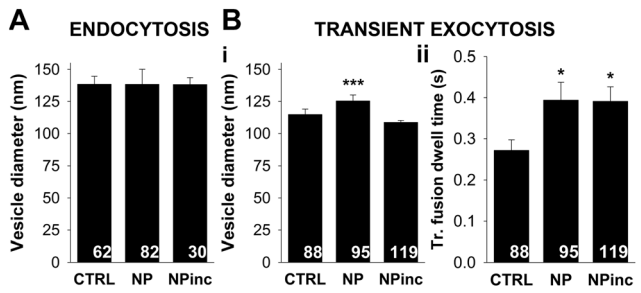

Fig. 2 The effect of astrocyte treatment with NPs on the amplitude of discrete steps in C_m, proportional to the vesicle size. The diameter of endocytotic vesicles (A) and transient exocytotic vesicles (Bi) with fusion pore dwell time (Bii), as calculated from the amplitude of discrete steps in C_m, assuming spherical morphology and a specific membrane capacitance of 8 fF μm^{-2}. Single astrocytes were either: cultured in regular medium (CTRL); cultured in regular medium and exposed to NPs in the patch-pipette solution during the recording (NP) or incubated for 24 h with NPs and then recorded in extracellular solution (ECS) (NPinc). Values are presented as means ± SEM. Significant differences between the groups are denoted as *P < 0.05, ***P < 0.001 compared with CTRL or between experimental groups, tested with ANOVA. The numbers in the columns represent the number of events analysed.

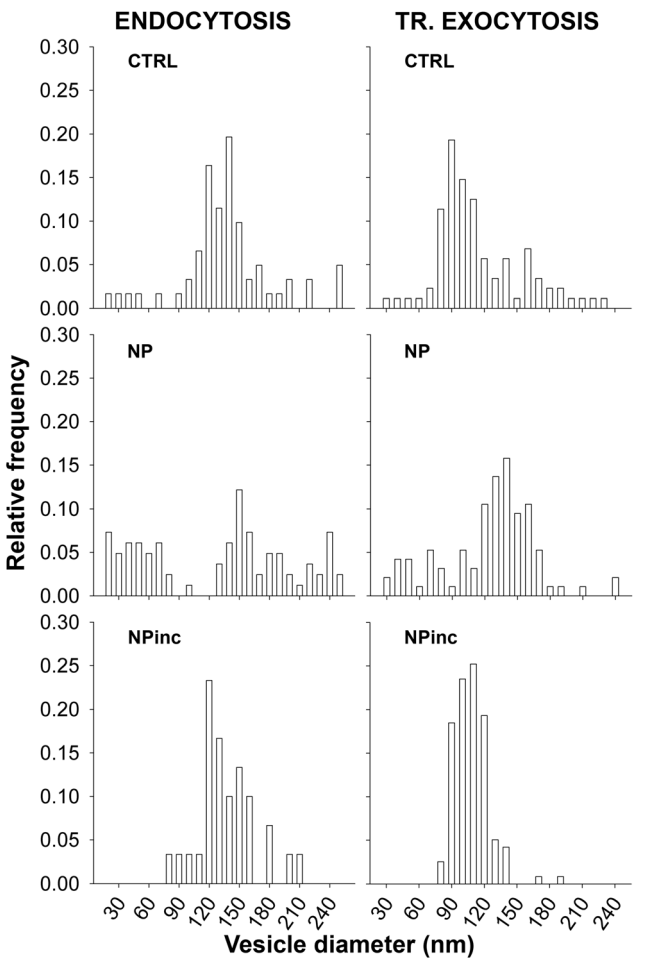

Fig. 3 Frequency distribution of endocytotic and exocytotic vesicle size. Distribution of endocytotic and exocytotic vesicle diameter recorded in single astrocytes: cultured in regular NP-free medium (CTRL), when exposed directly to NPs in the patch pipette (NP) and after 24 h of incubation with NPs (NPinc). The diameters were calculated from the amplitude of vesicle capacitance, assuming spherical morphology and a specific membrane capacitance of 8 fF μm^{-2}.

in vesicle size distribution from a peak vesicle diameter of 120–140 nm in controls to more or less equally distributed vesicle diameters ranging in size from 20 to 260 nm in cells acutely exposed to NPs, indicating that the presence of NPs in the extracellular space influences the size of the endocytotic vesicles.

Interestingly, with regard to possible NP recycling to the extracellular media after acute exposure of astrocytes to NPs and their internalization, an increase in the size of vesicles interacting with the plasma membrane (125 ± 5 nm, compared with 115 ± 4 nm in control astrocytes; $P < 0.001$; Fig. 2Bi) was found, although after 24 h of NP incubation, the average vesicle diameter was similar to controls (108 ± 2 nm). However, once astrocytes were exposed to NPs, vesicle interaction with the plasma membrane (fusion pore dwell time) was altered and exhibited similar properties as in astrocytes exposed acutely to NPs for a prolonged time (NPinc; Fig. 2Bii). This indicates that NPs exert long-lasting changes in astrocyte function, even when they are no longer in direct contact with the membrane where discrete vesicle fusions/fissions are recorded (within the lumen of the patch pipette). These results are also consistent with the frequency of vesicle diameter distribution histograms (Fig. 3, right panels) and suggest that acute NP exposure initiates exocytosis of larger vesicles. The results also indicate that 24 h after incubation, NPs may be cleared from the astrocytes within smaller vesicles probably as a result of cargo release and/or particle degradation within the astrocytes.

Fusion pore dwell time corresponds to the time a fusion pore stays open. Both acute and prolonged exposures to NPs have influenced fusion pore dwell time, revealing more stable and longer-lasting transient fusion pores in the presence of NPs and after they have been removed. Compared with the dwell times of basal astrocyte vesicles (272 ± 25 ms), both instant exposure to NPs and the longer incubation considerably increased the fusion pore dwell times (394 ± 44 ms and 391 ± 35 ms, respectively, Fig. 2Bii).

Overall, from the membrane capacitance measurements we were able to detect alterations in the frequency, diameter and pore fusion dwell time of astrocytic vesicles interacting with the plasma membrane when the NPs were acutely present or after exposure. One of the major advantages of this technique is the real-time monitoring of events in the live-cell membrane, which is extremely relevant for biological applications and can contribute to a more targeted design of NPs.

3.4. Co-localization experiments confirm sustained NP inward vesicular transport

Based on the reported NP hydrodynamic diameter and zeta potential,[26] and the calculated endosome diameter (Fig. 2A and 3), it is possible that a significant fraction of NPs is internalized into astrocytes through macropinocytosis. Nevertheless, other types of endocytosis cannot be excluded. To further test this hypothesis, pulse-chase experiments were performed by adding fluorescently labelled dextrans exogenously to astrocytes to allow the identification of endosomes.[8] Simultaneously, fluorescein isothiocyanate (FITC)-labelled NPs were added to astrocytes for different time periods to track intracellular trafficking of internalized NPs. Confocal live imaging revealed extensive FITC-labelled NP uptake, particularly over a 24-hour incubation period (Fig. 4A and S4†). Co-localization of NPs with dextrans demonstrated directly that NPs were internalized into endosomes.[8] Regardless of the NP

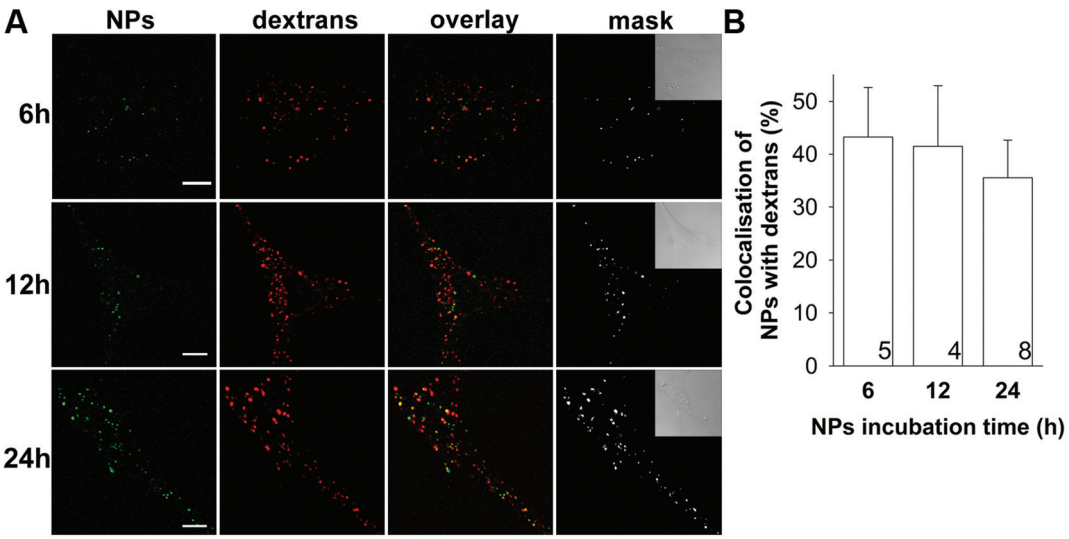

Fig. 4 Time-dependent co-localization of NPs with endocytotic dextran-labelled compartments in astrocytes. (A) Representative confocal micrographs of live astrocytes after Alexa Fluor 546-dextran labelling of macropinosomes (dextrans, red) and incubation with FITC-labelled *CM*Cht/PAMAM dendrimer NPs (NPs, green). Co-localization can be seen in yellow (overlay) and was extracted as white pixels (mask). Transmission light images of cells are presented in the insets. Three different NP incubation times were investigated: 6, 12 and 24 h. Scale bars represent 10 μm. (B) Relative co-localization of NPs with the dextran-labelled macropinosomes (in %), relative to all above threshold pixels of fluorescent NPs in the cells, at different incubation times of cells with NPs. Threshold was set to 20%. Error bars denote SEM; the numbers in the columns indicate the number of cells tested.

incubation times (6, 12, and 24 h), a similar percentage (43 ± 9% at 6 h; 42 ± 11% at 12 h; and 36 ± 7% at 24 h incubation) of co-localization of NPs with endosomal marker dextran was always observed (Fig. 4B), indicating rapid and persistent uptake of NPs into astrocytic compartments.

The time-independent co-localization between NPs and dextrans is likely attributable to a saturation effect, and also to endocytotic recycling regulatory mechanisms that control the membrane composition.[27] The initial rate of NP uptake is vital when considering clinical therapeutic applications, and here we have shown that dendrimer NPs are able to efficiently enter and remain internalized inside the astrocytes.

3.5. Live confocal vesicle tracking confirmed NP endocytotic compartments merge with secretory vesicles destined for exocytotic clearance

Next, we tested whether secretory vesicles destined for the exocytotic pathway, which appears to be stimulated by NP application (Fig. 1), co-localize with internalized NPs. Astrocytes were transfected with the plasmid encoding the fluorescently labelled mCherry-neuropeptide Y (NPY). NPY is a neuromodulator released *via* the exocytotic pathway from astrocytes,[28] commonly used in regulated secretion assays.[29] Co-localization of FITC-labelled NPs with mCherry-NPY exocytotic vesicles was detected at all time intervals tested, indicating that the NPs that enter the astrocytes may merge with vesicles destined for exocytotic release. However, the experiments revealed that the merger between the internalized NPs with NPY compartments is a time-dependent process, because a plateau at the level of merger was observed 12 h after incubation with the NPs (Fig. 5). Co-localization after incubation for 6 h was 14 ± 4% (n = 10), and after 12 h and 24 h incubation, co-localization levels of 38 ± 10% and 40 ± 6%, respectively, were significantly higher (P = 0.04 and P = 0.008, respectively, Fig. 5A and S5†). These results are consistent with our electrophysiological data; both showing that the treatment of cells with the NPs does not coincide with an increased rate of exocytosis, but rather that the rate of exocytosis and merger of NPs with the exocytotic pathway slowly increase to maximal values after incubation with NPs for 12 h. For the first time, these results reveal that the *CM*Cht/PAMAM dendrimer NPs, once taken up into a cell, may merge with the secretory vesicles destined for exocytotic release.

3.6. NP trafficking in astrocytes after 1 week of incubation

Time is a key factor in putative NP-related biomedical applications, especially the long-term fate of internalized NPs. To test how long NPs persist in the astrocytes once they are internalized, we maintained cortical astrocytes for a week after incubation with NPs for 24 h. The culture medium was changed every day for a week (without the presence of NPs) to continuously wash the remaining NPs putatively released from the astrocytes (Fig. 6). Endocytotic and exocytotic vesicles were labelled with Alexa Fluor 546 dextrans and mCherry-NPY, respectively. Live astrocyte cultures were observed under a confocal microscope. As noted in Fig. 6, FITC-labelled NPs were present for 24 h in the astrocyte cultures. Nonetheless, very modest co-localization with endosomes (dextrans) was quantified after a week (15 ± 2%), and was significantly reduced compared with their presence immediately after incubation for

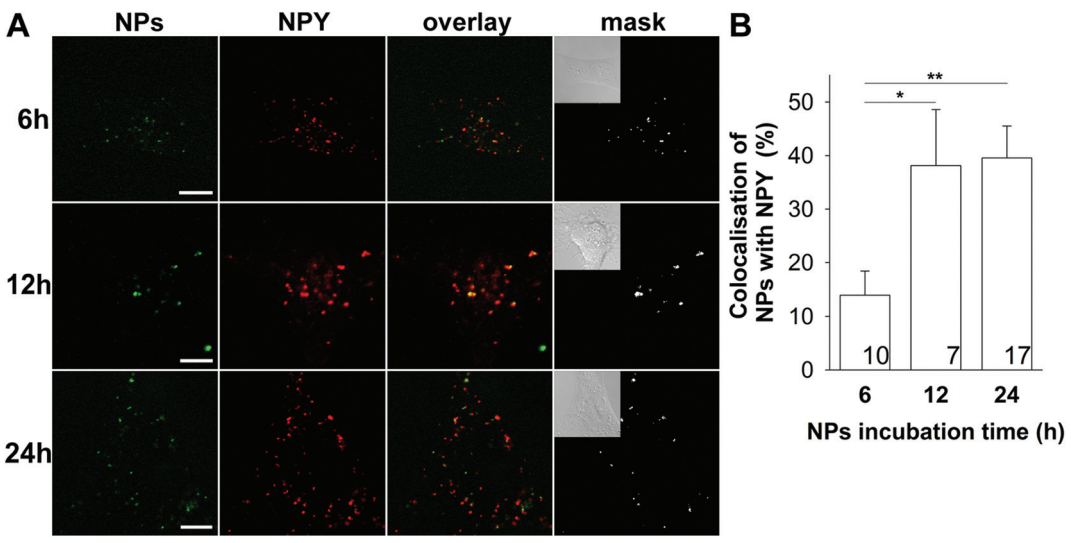

Fig. 5 Time-dependent co-localization of NPs with exocytotic mCherry-NPY-labelled vesicles in astrocytes. (A) Representative confocal micrographs of live astrocytes: labelled exocytotic vesicles with mCherry-NPY (NPY, red) and incubated with FITC-labelled *CM*Cht/PAMAM dendrimer NPs (NPs, green). Co-localization can be seen in yellow (overlay) and was extracted as white pixels (mask). Transmission light images of cells are presented in the insets. Three different times of incubation with NPs were investigated: 6, 12 and 24 h. Scale bars represent 10 μm. (B) Relative co-localization of NPs with the NPY-labelled exocytotic vesicles (in %), relative to all above threshold pixels of fluorescent NPs in the cell, at different incubation times of cells with NPs. Threshold was 20%. Error bars denote SEM; the numbers in the columns indicate the number of cells tested; asterisks denote statistically significant difference tested with ANOVA (*P < 0.05; **P < 0.01).

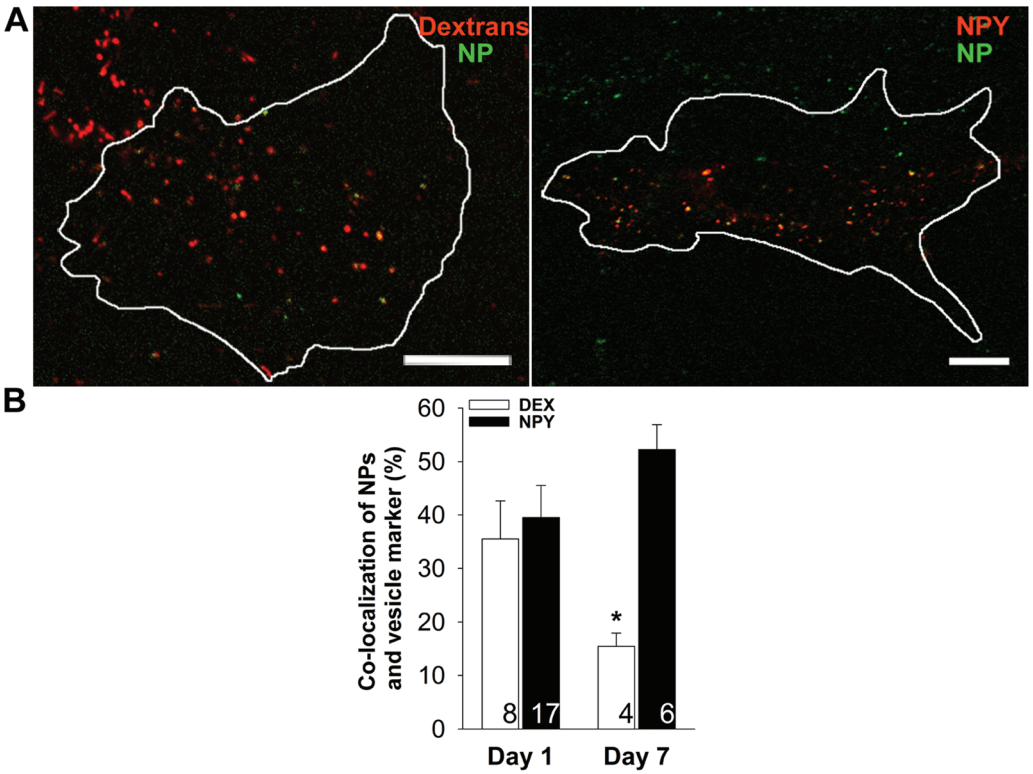

Fig. 6 Co-localization of NPs with fluorescently labelled subcellular compartments 1 week after NP exposure in astrocytes. (A) Confocal micrographs of live astrocytes after Alexa Fluor 546 dextran incubation (left panel, macropinosomes in red) and mCherry-NPY transfection (right panel, exocytotic vesicles in red) 7 days after NP exposure. FITC-labelled *CM*Cht/PAMAM dendrimer NPs (in green) were incubated for 24 h and then removed from the medium, with daily medium change for 1 week. Co-localizations can be seen in yellow. Scale bars represent 10 μm. (B) Co-localization coefficient of NPs with membrane vesicles in % with the Alexa Fluor 546 dextran-labelled macropinosomes (Dex, white bars) and with the mCherry-NPY-labelled vesicles (NPY, black bars), after 1 day incubation with NPs or after 7 days. Error bars indicate SEM; the numbers in the columns indicate the number of cells analysed. Significant differences compared with the respective day 1 are denoted as $*P < 0.05$ (Student's *t* test).

24 h (36 ± 7%). On the other hand, co-localization of NPs with NPY-positive secretory vesicles increased from 40 ± 6% (n = 17) at day 1 to 52 ± 5% (n = 6) after 7 days. These results strongly indicate that the process of merger between endocytotic and secretory vesicles containing the NPs is long lived; it persists 1 week after exposure of astrocytes to NPs. During this period, the retention of NPs in the endocytotic compartment is greatly reduced, likely because the endosomal NP content is transferred to secretory vesicles.

These results indicate that dendrimer NPs follow the typical intracellular trafficking pathways, namely endocytotic (with emphasis on macropinocytosis) and exocytotic routes.

4. Discussion

It is only very recently that the pathological significance of neuroglia has been acknowledged.[30–35] Astrocytes outnumber neurons in the neocortex, the largest structure of the human brain with a mass exceeding 80% of the brain, where they perform a variety of important functions.[35–38] In principle, as with any other disease, neurological diseases result from a homeostatic failure. However, it is the neuroglia that provides full homeostatic and neuroprotective support. Thus, neuroglial cells, especially astrocytes, have an important role in defining the CNS defence against alterations leading to neurological diseases, including neurodegeneration. Astrocytes also contribute to the evolution of neurodegeneration through alterations in vesicle traffic.[39,40] Therefore, astrocytes are not just ideal targets but also crucial targets in therapies for CNS disorders after trauma or degenerative progression.[41–43]

Here, we studied the interaction of NPs with astrocytes. *CM*Cht/PAMAM dendrimer NPs have many attractive features that render them promising nanocarrier candidates to be used in biomedical applications, namely in CNS disorders.[12–15] *CM*Cht/PAMAM dendrimer NPs have already been tested in neuroinflammation models. *In vitro* and *in vivo* experiments have shown that *CM*Cht/PAMAM dendrimer NPs are biocompatible in primary nerve cell cultures and cause no toxicity in rat models after intravenous or local administration,[14,15] however the mechanisms underlying the interaction of these NPs with cells remain unclear. Here the interaction of NPs with astrocytes has been studied directly. NP intracellular trafficking and clearance routes have been investigated in astrocytes using cell-attached patch-clamp electrophysiology. Discrete alterations in the membrane capacitance (C_m) were

monitored, which reflect unitary endocytotic and exocytotic events and allow for monitoring the frequency of vesicle formation/fusion and the calculation of vesicle diameter and fusion pore opening time.[44] In addition, confocal imaging in live astrocytes after incubation with fluorescently labelled NPs and vesicle-staining dyes enabled us to track co-localization, corroborating NP vesicular transport.

Astrocytes, like other eukaryotic cells, contain secretory vesicles with varied diameter and are suitable for vesicle luminal cargo release, as for the delivery of membrane-associated receptors to the plasma membrane.[45–48] Compared with neurons, the kinetics of exocytosis was shown to be slower in astrocytes[49] with several types of discrete vesicle interactions with the plasma membrane[24,50] as recorded in this study. The interaction of NPs with the plasma membrane and especially how NPs modify merging of the unitary vesicle with the plasma membrane have not been carried out but are important in relation to intracellular retention and possible clearance of NPs. These parameters are critical when considering therapeutic applications using NPs.[25,51–53]

We show here that the presence of NPs tends to increase the rate of endocytosis; however no significant level of this increase was demonstrated (Fig. 1). When NPs are in close vicinity to a cell, the interactions between the NPs and the cell membrane generate forces from different origins. This leads to membrane wrapping of the NPs followed by cellular uptake. This is then influenced by the shape, size, surface chemistry and stiffness of NPs as well as by the micro-environment (reviewed by Zhang *et al.*).[54] Also, the vesicle diameter was on average the same as in controls (Fig. 2), but the variation of endocytotic vesicle diameter profile was observed (Fig. 3), indicating that the cells detect and react to the presence of NPs in the milieu. Non-modified PAMAM dendrimers have recently been reported to follow different endocytotic pathways to enter cells,[8,55] from receptor-mediated endocytosis (*e.g.* clathrin-mediated endocytosis) to other non-specific uptake routes such as macropinocytosis, depending on dendrimer generation and surface properties.[56] *CM*Cht-grafted PAMAM dendrimers have been suggested to follow unspecified endocytotic routes.[13] However, studies involving inhibitors of endocytosis have shown that inhibitors are not selective, influencing more than a single pathway.[57] Therefore, complementary methods are crucial to better understand the mechanisms of cellular NP trafficking.

Vesicle formation rates obtained from C_m readings do not allow discrimination and identification of specific endocytotic routes. Notwithstanding, the vesicle size can be associated with specific endocytotic pathways, *e.g.* larger molecules tend to be internalized by macropinosomes, and consequently by larger vesicles.[58] Moreover, the patch-clamp technique allows quantification of additional vesicle parameters (such as fusion pore opening time) providing further insights into the characteristics of the trafficking pathway being activated.

Combining quantitative and qualitative data obtained from patch-clamp electrophysiology and live-cell confocal imaging has been shown to be appropriate and relevant in the study of endocytotic and exocytotic mechanisms, and has provided valuable and reliable information on the uptake and fate of NPs in astrocytes. Confocal imaging confirmed the important contribution of macropinocytosis in the endocytotic uptake of dendrimer NPs (>40%, Fig. 4) and the time dependence of this process (Fig. 4). The presence of NPs did not influence the rate of exocytosis, however after wash-out of NPs, a significant increase of exocytotic occurrence was detected in cells incubated for 24 h with NPs, more specifically a predominant (Table 1, ESI†), transient type of exocytosis (Fig. 1Biii). This increase in exocytotic activity and also an increased fusion pore dwell time (Fig. 2Bii) suggest that at that point NPs tend to be extensively cleared out from the cells. The exocytotic vesicle diameter is increased at the acute NP exposure (Fig. 2Bi) compared to controls. This could be due to several reasons, but most probably this reaction is triggered by the physical presence of NPs. Live imaging of the cells has demonstrated that NPs are located inside exocytotic vesicles within 6 h after exposure (Fig. 5) and are increasingly delivered to this compartment at least for 1 week after incubation (Fig. 5 and 6), showing that this is a continuous and dynamic clearance process. Expectedly, endocytosis drastically decreased at this point compared with 24 hours after NP exposure (Fig. 6). These results provide new insights into the interaction of NPs with astrocytes, in relation to the recycling mechanisms. Particularly, they demonstrate the uptake and clearance route of drug-loaded dendrimer NPs to follow the classical membrane recycling pathway and are eventually cleared from the cells. No deleterious effects were observed during NP trafficking, confirming the potential biomedical applicability of these intracellular nanocarriers. In addition, this study has demonstrated the potential relevance of patch-clamp measurements for studies involving nanomaterials and cell membrane interaction studies, given the in-depth knowledge provided.

5. Conclusions

In summary, the results reveal that dendrimer NPs are taken up by endocytosis into astrocytes, and this is followed by an increase in the frequency of transient exocytotic fusion events that exhibit a longer fusion pore dwell time, which may be indicative of the cell clearance process of NPs. Co-localization imaging studies showed a time-dependent increase in the clearance process of NPs through exocytotic vesicles. The original combination of the techniques used herein can benefit future studies in the field by providing insightful information on NP–cell membrane interaction and intracellular trafficking, as well as clearing.

Conflicts of interest

The authors declare no competing financial interest.

Acknowledgements

This study was supported by the Slovenian Research Agency (grants P3 310, J3 6790, and J3 7605) and the European Science Foundation COST STSM grant attributed to S. R. Cerqueira. The authors would also like to acknowledge the funds from the Portuguese Foundation for Science and Technology (fellowship to S. R. C. SFRH/BD/48406/2008) and the European Union's Seventh Framework Programme (FP7/2007-2013, grant agreement no. REGPOT-CT2012-316331-POLARIS). J. M. O. also acknowledges the FCT for the funds provided under the program Investigador FCT (IF/00423/2012 and IF/01285/2015).

References

1 A. R. Menjoge, R. M. Kannan and D. A. Tomalia, *Drug Discovery Today*, 2010, **15**, 171.
2 D.-E. Lee, H. Koo, I.-C. Sun, J. H. Ryu, K. Kim and I. C. Kwon, *Chem. Soc. Rev.*, 2012, **41**, 2656.
3 A. Z. Wilczewska, K. Niemirowicz, K. H. Markiewicz and H. Car, *Pharmacol. Rep.*, 2012, **64**, 1020.
4 W. H. De Jong and P. J. Borm, *Int. J. Nanomed.*, 2008, **3**, 133.
5 J. M. Oliveira, A. J. Salgado, N. Sousa, J. F. Mano and R. L. Reis, *Prog. Polym. Sci.*, 2010, **35**, 1163.
6 S. Svenson and D. A. Tomalia, *Adv. Drug Delivery Rev.*, 2012, **57**, 2106.
7 D. Astruc, E. Boisselier and C. Ornelas, *Chem. Rev.*, 2010, **110**, 1857.
8 L. Albertazzi, M. Serresi, A. Albanese and F. Beltram, *Mol. Pharm.*, 2010, **7**, 680.
9 X. Duan and Y. Li, *Small*, 2013, **9**, 1521.
10 O. P. Perumal, R. Inapagolla, S. Kannan and R. M. Kannan, *Biomaterials*, 2008, **29**, 3469.
11 L. Treuel, X. Jiang and G. U. Nienhaus, *J. R. Soc., Interface*, 2013, **10**, 20120939.
12 S. R. Cerqueira, B. L. Silva, J. M. Oliveira, J. F. Mano, N. Sousa, A. J. Salgado and R. L. Reis, *Macromol. Biosci.*, 2012, **12**, 591.
13 J. M. Oliveira, N. Kotobuki, A. P. Marques, R. P. Pirraco, J. Benesch, M. Hirose, S. A. Costa, J. F. Mano, H. Ohgushi and R. L. Reis, *Adv. Funct. Mater.*, 2008, **18**, 1840.
14 S. R. Cerqueira, J. M. Oliveira, N. A. Silva, H. Leite-Almeida, S. Ribeiro-Samy, A. Almeida, J. F. Mano, N. Sousa, A. J. Salgado and R. L. Reis, *Small*, 2013, **9**, 738.
15 V. H. Pereira, A. Salgado, J. M. Oliveira, S. R. Cerqueira, A. Frias, J. Fraga, S. Roque, A. M. Falcão, F. Marques and N. Neves, *J. Bioact. Compat. Polym.*, 2011, **26**, 619.
16 M. Pojo, S. R. Cerqueira, T. Mota, A. Xavier-Magalhães, S. Ribeiro-Samy, J. F. Mano, J. M. Oliveira, R. L. Reis, N. Sousa, B. M. Costa and A. J. Salgado, *J. Nanopart. Res.*, 2013, **15**, 1621.
17 E. Neher and A. Marty, *Proc. Natl. Acad. Sci. U. S. A.*, 1982, **79**, 6712.
18 B. Rituper, A. Guček, J. Jorgačevski, A. Flašker, M. Kreft and R. Zorec, *Nat. Protoc.*, 2013, **8**, 1169.
19 M. Gabrijel, M. Kreft and R. Zorec, *Biochim. Biophys. Acta*, 2008, **1778**, 483.
20 J. P. Schwarts and D. J. Wilson, *Glia*, 1992, **5**, 75.
21 M. Lindau and E. Neher, *Pflugers Arch.*, 1988, **411**, 137.
22 A. J. Salgado, J. M. Oliveira, R. P. Pirraco, V. H. Pereira, J. S. Fraga, A. P. Marques, N. M. Neves, J. F. Mano, R. L. Reis and N. Sousa, *Macromol. Biosci.*, 2010, **10**, 1130.
23 J. Jorgačevski, M. Stenovec, M. Kreft, A. Bajić, B. Rituper, N. Vardjan, S. Stojilkovic and R. Zorec, *Am. J. Physiol.: Cell Physiol.*, 2008, **295**, C624.
24 A. Gucek, J. Jorgacevski, P. Singh, C. Geisler, M. Lisjak, N. Vardjan, M. Kreft, A. Egner and R. Zorec, *Cell. Mol. Life Sci.*, 2016, **73**, 3719.
25 J. Panyam and V. Labhasetwar, *Pharm. Res.*, 2003, **20**, 212.
26 M. C. Kerr and R. D. Teasdale, *Traffic*, 2009, **10**, 364.
27 B. D. Grant and J. G. Donaldson, *Nat. Rev. Mol. Cell Biol.*, 2009, **10**, 597.
28 P. Ramamoorthy and M. D. Whim, *J. Neurosci.*, 2008, **28**, 13815.
29 I. Grigoriev, K. L. Yu, E. Martinez-Sanchez, A. Serra-Marques, I. Smal, E. Meijering, J. Demmers, J. Peränen, R. J. Pasterkamp, P. van der Sluijs, C. C. Hoogenraad and A. Akhmanova, *Curr. Biol.*, 2011, **21**, 967.
30 J. E. Burda and M. V. Sofroniew, *Neuron*, 2014, **81**, 229.
31 A. Verkhratsky, J. J. Rodriguez and V. Parpura, *Future Neurol.*, 2013, **8**, 149.
32 A. Verkhratsky, M. V. Sofroniew, A. Messing, N. C. deLanerolle, D. Rempe, J. J. Rodriguez and M. Nedergaard, *ASN Neuro*, 2012, **4**, 3.
33 J. De Keyser, J. P. Mostert and M. W. Koch, *J. Neurol. Sci.*, 2008, **267**, 3.
34 M. Pekny, M. Pekna, A. Messing, C. Steinhauser, J. M. Lee, V. Parpura, E. M. Hol, M. V. Sofroniew and A. Verkhratsky, *Acta Neuropathol.*, 2016, **131**, 323.
35 V. Parpura, M. T. Heneka, V. Montana, S. H. Oliet, A. Schousboe, P. G. Haydon, R. F. Stout Jr., D. C. Spray, A. Reichenbach, T. Pannicke, M. Pekny, M. Pekna, R. Zorec and A. Verkhratsky, *J. Neurochem.*, 2012, **121**, 4.
36 M. Potokar, N. Vardjan, M. Stenovec, M. Gabrijel, S. Trkov, J. Jorgačevski, M. Kreft and R. Zorec, *Int. J. Mol. Sci.*, 2013, **14**, 11238.
37 M. Nedergaard, B. Ransom and S. Goldman, *Trends Neurosci.*, 2003, **26**, 523.
38 A. S. Thrane, V. Rangroo Thrane and M. Nedergaard, *Trends Neurosci.*, 2014, **37**, 620.
39 M. Stenovec, S. Trkov, E. Lasič, S. Terzieva, M. Kreft, J. J. Rodríguez Arellano, V. Parpura, A. Verkhratsky and R. Zorec, *Glia*, 2016, **64**, 317.
40 R. Zorec, V. Parpura and A. Verkhratsky, *Neurochem. Res.*, 2017, **42**, 905.
41 H. K. Kimelberg and M. Nedergaard, *Neurotherapeutics*, 2010, **7**, 338.
42 E. M. Hol and M. Pekny, *Curr. Opin. Cell Biol.*, 2015, **32**, 121.
43 A. Verkhratsky and V. Parpura, *Neurobiol. Dis.*, 2016, **85**, 254.

44 J. M. Fernandez, E. Neher and B. D. Gomperts, *Nature*, 1984, **312**, 453.
45 A. Guček, N. Vardjan and R. Zorec, *Neurochem. Res.*, 2012, **37**, 2351.
46 A. Verkhratsky, M. Matteoli, V. Parpura, J. P. Mothet and R. Zorec, *EMBO J.*, 2016, **35**, 239.
47 N. Vardjan, A. Verkhratsky and R. Zorec, *Cell Transplant.*, 2015, **24**, 599.
48 N. Vardjan and R. Zorec, *Neurochem. Res.*, 2015, **40**, 2414.
49 M. Kreft, M. Stenovec, M. Rupnik, S. Grilc, M. Krzan, M. Potokar, T. Pangrsic, P. G. Haydon and R. Zorec, *Glia*, 2004, **46**, 437.
50 E. Lasic, B. Rituper, J. Jorgacevski, M. Kreft, M. Stenovec and R. Zorec, *J. Neurochem.*, 2016, **138**, 909.
51 D. Bartczak, S. Nitti, T. M. Millar and A. G. Kanaras, *Nanoscale*, 2012, **4**, 4470.
52 X. Jiang, C. Röcker, M. Hafner, S. Brandholt, R. M. Dörlich and G. U. Nienhaus, *ACS Nano*, 2010, **4**, 6787.
53 Y. Wang, Q. Wu, K. Sui, X.-X. Chen, J. Fang, X. Hu, M. Wu and Y. Liu, *Nanoscale*, 2013, **5**, 4737.
54 S. Zhang, H. Gao and G. Bao, *ACS Nano*, 2015, **9**, 8655.
55 G. Sahay, D. Y. Alakhova and A. V. Kabanov, *J. Controlled Release*, 2010, **145**, 182.
56 K. M. Kitchens, R. B. Kolhatkar, P. W. Swaan and H. Ghandehari, *Mol. Pharm.*, 2008, **5**, 364.
57 A. I. Ivanov, *Methods Mol. Biol.*, 2008, **440**, 15.
58 T.-G. Iversen, T. Skotland and K. Sandvig, *Nano Today*, 2011, **6**, 176.